Journal of Materials and Engineering Structures

Research Paper

Protection of structures subject to seismic and mechanical vibrations using periodical networks

Amine Amrane [a,*], Nouredine Bourahla [a], Abdelkader Hassein-Bey [b], Abedelkrim Khelif [c]

[a] *Departement of Civil Engineering, Faculty of Technology, Blida 1 University, Algeria.*

[b] *Departement of Physics (Micro & Nano Systems), Faculty of Sciences, Blida 1 University, Algeria.*

[c] *Institut FEMTO-ST, CNRS UMR 6174, Université de Franche-Comté, 32 avenue de l'Observatoire, 25044 Besançon Cedex, France.*

ARTICLE INFO

Article history :

Received : 30 June 2018

Revised : 25 November 2018

Accepted : 4 December 2018

Keywords:

Band gap in civil engineering

Isolation of structures

Phononic Structures

ABSTRACT

The concept of frequency gaps in phononic crystals is widely used in physics. The feasibility and efficiency of applying this principle in damping out seismic and mechanical induced vibrations in real scale of civil engineering constructions are presented in this article through the results obtained from numerical modeling and analysis of a concrete substratum embedding steel elements (pillars) coated in a polyvinyl chloride polymer (PVC). The first configuration having the elements fully embedded into the substrate resulted in two narrow band gaps at relatively high frequencies; and when only the metallic pillars are emerging from the substrate, the band gaps shift towards the low frequencies. The results are improved and show the existence of three band gaps at medium frequencies ranging from 80 to 200 m/s when both the pillars and the polymer are emerging from the foundation. Exploring other metal-polymer pairs of materials such as "steel-rubber", "steel-silicone"," lead-rubber" and "lead-silicone", shows that a range of band gaps has shifted again towards the lower frequencies which cover part of the seismic frequency domain. Further improvement is obtained by notching the ends of the substrate in order to widen and lower the band gaps especially for "metal-rubber" pairs. For the couple of materials "steel-silicone", the width of band gap is expanded as the thickness of silicone layer is decreased from 10 to 5 and to 2.5 cm. These results show the potential of using periodic networks to mitigate seismic and mechanical vibration effects on large scale structures and components.

1 Introduction

The loss of lives and collapse of buildings caused by severe earthquakes have motivated researchers to develop different techniques and measures to mitigate the structural and non structural damage. Different conventional seismic isolators

* *Corresponding author. Tel.: +213 664 754 489.*
E-mail address: amine.amrane@univ-blida.dz

e-ISSN: 2170-127X,

RESEARCH REVIEW of Sciences and Technologies

systems for civil engineering structures have been introduced a long time ago, and continue to be improved in many aspects [1-9].

New approaches such as the one proposed by Li et al.[10] provides an efficient method to construct a negative stiffness vibration isolator for practical use for components.

The researchers present a negative stiffness magnetic suspension vibration isolator (NSMSVI) using a magnetic spring in combination with rubber membranes. They have shown that a magnetic spring acts in repulsion with positive stiffness, whereas the negative stiffness is achieved by the rubber membrane. The isolator could obtain low natural frequency as the positive stiffness is partly counteracted by negative stiffness. They have shown also that the vibration isolation performance of a passive vibration isolator in low input frequencies is considerably improved by reducing its natural frequency.

Recently, an innovative approach based on periodical networks has been proposed by several researchers. In fact, the phenomenon of band gaps which was previously confined only to solid state physics and semiconductors has been extended to other vibration phenomena. In the latter extensive research works has been conducted by different authors [11-17] and have demonstrated the existence of forbidden frequency bands which prevent the propagation of certain acoustic frequencies and therefore can be used as filters in communication systems and as acoustic isolators for resonant sensors such as gyroscopes.

The study of acoustic and elastic wave propagation in phononic crystals has been receiving great interest recently. Hsiao et al. and Pennec et al. [18-19] have studied phononic crystals which are inhomogeneous elastic media composed of one, two, or three dimensional periodic arrays of inclusions embedded in a matrix.

Some authors [20-22] have concluded that phononic band gaps (PBGs) can be used to realize fundamental functionalities such as mirroring, guiding, entrapment, and filtering of acoustic/elastic waves by creating defects in the phononic cristals (PC) structures; they have also concluded that these structures have a high potential use as energy loss reduction in micromechanical resonators at high frequency regime.

Using the same concept of frequency band gaps in periodic materials, some researchers [23-25] proposed some innovative insulating phononic networks capable to mitigate structural damage of buildings subjected to earthquake or mechanical vibrations.

Elastic waves exist over a very wide range of frequencies; they range from Hz in the case of seismic waves to GHz for telecommunication networks.

However, to obtain band gaps due only to the Bragg diffraction in the field of civil engineering is a challenging task because of the very low frequency range of the structures and the length of seismic waves which would require very large dimensions of periodic structures acting as isolators in order to be efficient. Several attempts have been made by several researchers to overcome this obstacle. In this context, some researchers [26-30] examined the potential of the local resonance phenomenon using semi-infinite substrates on which were put up cylindrical pillars. They concluded that some dispersion came from resonance of local vibration modes. Recently, more research works were conducted on concrete foundations and buildings containing phononic networks. The Results of numerical simulation conducted by these authors [24] show that periodic foundations have a great potential in future application in seismic isolation.

A foundation block of a small scale model of a building made of alternated rubber layers has been studied by Xiang et al. [12]. The authors have shown experimentally that for this particular case a range of seismic frequencies could be totally blocked or deflected.

Thin slabs with step resonators have been used to demonstrate that simultaneous effect of the local resonance phenomena and Bragg diffraction led to low frequency band gaps. Hsu [25] has also confirmed that by varying the geometric parameters, these band gaps could be extended.

In a very recent work conducted by Wagner et al. [31] which investigated the possibility of using metamaterials in seismic isolation. The results show that using metamaterials can mitigate the seismic vibrations.

From this perspective, this paper explores the possibilities to shift band gaps towards the range of the frequency content of seismic excitations and proposes an isolation base for an entire structure or part of it such as equipments, incorporating periodic arrays. The cell units of the base model are made of core cylinders coated with a polymer layer embedded in a concrete thin mat. The material characteristics of both the inner core cylinder and the coating layer are varied using

characteristics of real materials. The geometric characteristics of the cell unit parameters are also varied and combined with those of the mechanical characteristics in order to have a better insight of the effect of each parameter that contributes to wider the band gaps and to lower their central frequency to the range of interest.

This paper presents first the design of the model with some modelling and simulation considerations of the different materials then the analysis and results.

2 Model design and simulation

The model is a square concrete mat having a thickness "t" relatively small compared to its in plan dimensions. The mat is inlaid with columns (pillars) of circular sections coated by different materials in the embedded parts. The inner cylinders of the first basic sample are made of steel; and surrounded by a PVC layer as shown in Fig. 1(a). The basic unit in Fig. 1(b) is square having a dimension "*a*" representing the main dimension of the unit cell of the periodic array. PVC and steel columns have relative radius and relative heights (r_1/a; h_1/a) and (r_2/a; h_2/a) respectively. Different samples are derived where the steel is replaced by lead while the PVC is replaced by rubber and then by silicone. However, in the first time, the influence of the pillars height has been considered using two cases: the core and polymer have the same height as the substrate $h_1=h_2=h=t$ (Fig. 1(c)) and steel pillars emerge from the substrate of concrete ($h_1=t$ *and* h_2/a=0.5) as shown in Fig. 2(a).

In the second time, we consider metal core and polymer having the same relative height ($h_1/a= h_2/a$ =0.5) as illustrated in Figs. 1(a) and 1(b).

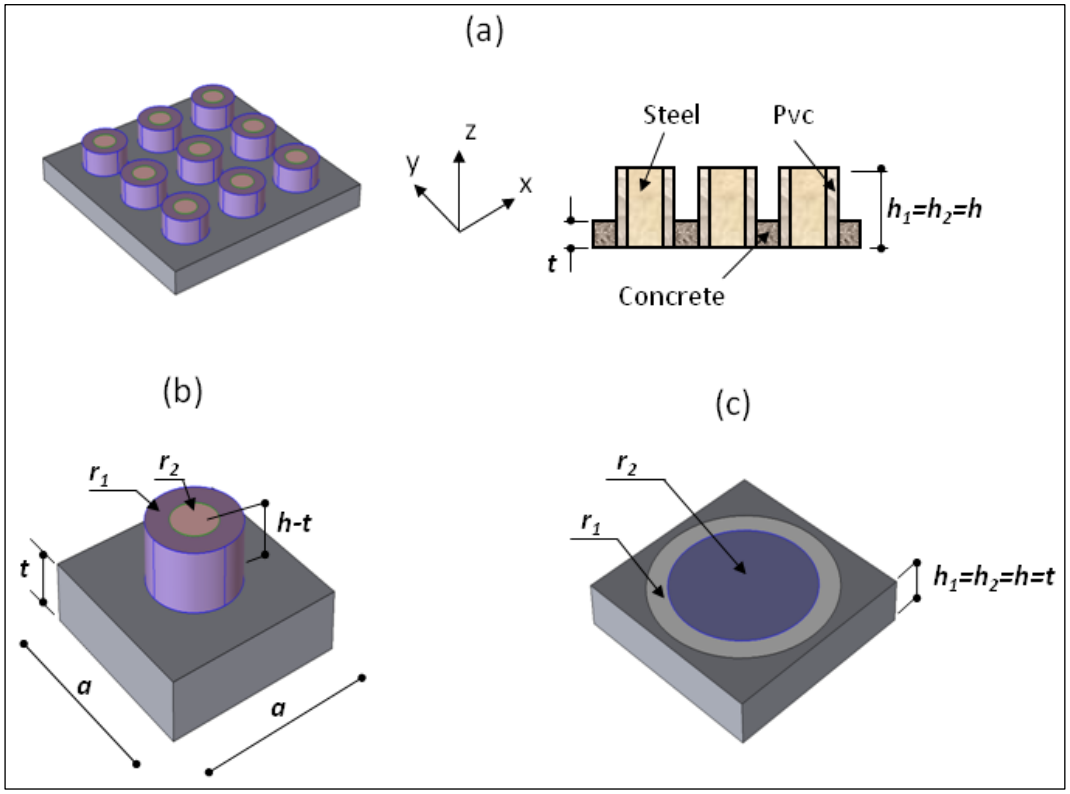

Fig. 1 – Solid concrete with a periodic network consisting of steel cylinders surrounded by a layer of PVC. (a) Model of structure is assumed to be infinite in both directions x and y. (b) Basic model in third phase (before notching) [32]. (c) Basic model in first phase (h1=h2=t)

However, four phases are considered. in the first one, the core and polymer have the same height as the substrate, $h_1=h_2=h=t$ (Fig. 2(a)). In the second phase, only steel emerge from the substrate of concrete, $h_1=t$ and h_2/a=0.5 (Fig.2(b)). In the third phase, steel and coated pillars emerge with the same height from the substrate of concrete, $h_1/a= h_2/a=0.5$ (Fig.2(c)). In the fourth phase, notches are making at the corners of the basic unit as shown in Fig.2(d).

Different samples are derived in third and fourth phases, where the steel is replaced by lead while the PVC is replaced by rubber and then by silicone [32].

The various models have been numerically studied using the finite element method (FEM). The mechanical properties of the different materials used in this study (density ρ, Longitudinal elastic modulus E, Poisson's ratio v and elasticity coefficients C_{11}, C_{12}, and C_{44}) are given in Table 1.

The dimensions of the structure are assumed infinite in both directions X and Y. The simulations focus on the primary base cell by applying the limit conditions Bloch-Floquet at the cell boundaries [32]. The mechanical displacements can be deduced for any nodes on the boundary with Bloch-Floquet theorem using Equations (1)-(3).

Table 1 - Material characteristics

	Density ρ (kg/m^3)	E (GPa)	v	C_{11} (GPa)	C_{12} (GPa)	C_{44} (GPa)
Concrete	2400	30	0.3	40.38	17.3057	11.538
Steel	7870	209	0.3	281.35	120.578	80.385
Lead	11350	16.7	0.44	54.12	42.5228	5.7986
PVC	1400	0.35	0.3	0.47	0.2014	0.1346
Rubber	950	0.1	0.45	0.379	0.3101	0.03448
Silicone	1300	0.000137	0.463	0.000679	0.000585	0.0000468

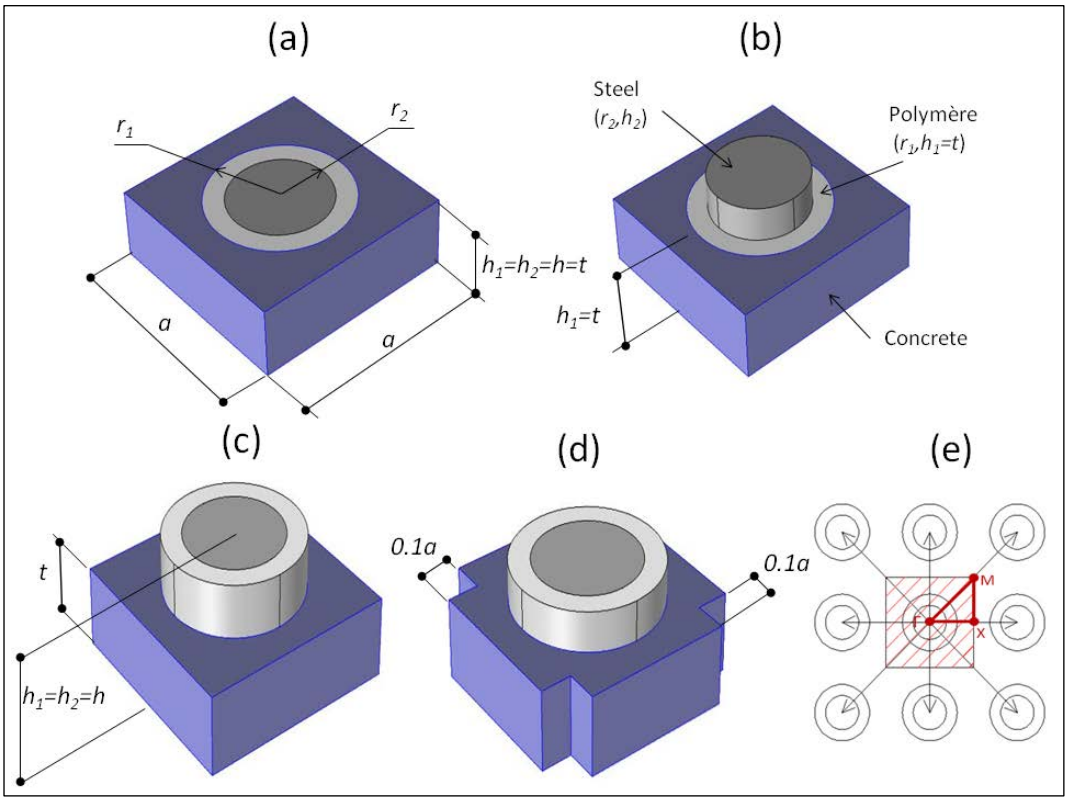

Fig. 2 – Basic models consist of concrete substrate with steel cylinders surrounded by a layer of PVC in all phases. (a) First phase ($h_1=h_2=t$). (b) Second phase ($h_1=t$ and $h_2/a=0.5$). (c) Third phase (before notching). (d) Fourth phase (after notching). (e) The first irreductible Brillouin zone (triangle ΓXM) in reciprocal space.

The periodicity of the structure and displacement allows the band of frequency gap to be investigated by studying one period, or unit cell. As result, the periodic boundary condition needs to be applied as illustrated by equation (1). For a square lattice, as shown in Fig. 2(d), the unit cell is hatched square.

The band of frequency gap of the system is obtained by solving for the Eigen frequencies of the system at different values of the Bloch wave vector ***k*** expressed as [k_x, k_y], which is defined in the reciprocal space and represents the excitation source of vibration and so represents different wave travelling directions.

Due to high symmetry of the first Brillouin zone, to obtain the band of the frequency gap for waves travelling in all directions ([0° , 360°]), it is sufficient to calculate only along the boundary of the first irreductible Brillouin zone, which is the triangle in Fig. 2(d). The triangle is denoted by ΓXM letters. This boundary can cover waves travelling directions of $\theta \in (0°, 45°)$; θ is the angle formed by ΓX and ΓM [33].

For example, k_x varies between (0,π/a) in ΓX direction (k_y=0); k_y varies between (0,π/a) in XM direction (k_x=π/a) and both k_x, k_y varie between (π/a,0) in MΓ direction.

$$u_i(x+a,y,z) = u_i = (x,y,z)e^{((i(a*kx)))} \tag{1}$$

A simple dynamic law is used to deduce harmonic wave equation, which is given by:

$$F = -\rho\omega 2u_i = \partial T_{ij}\partial X_{ij} \tag{2}$$

Where ρ is the density of material, ω is the angular frequency, u_i is the displacement in i direction.

The stress tensor T_{ij} can be related to strain S_{kl} by Hooke's Law and:

$$T_{ij} = C_{ijkl} \times S_{kj} \tag{3}$$

Where C_{ijkl} is the stiffness constant using Einstein summation convention for repeated indices.

The tensor of stresses and deformations can be written in Hooke law with α, β coefficients.

$$T_\alpha = C_{\alpha\beta} \times S_\beta \tag{4}$$

For an isotropic material, the elasticity matrix $C_{\alpha\beta}$ is equal to:

$$C_{\alpha\beta} = \begin{vmatrix} C_{11} & C_{12} & C_{12} & 0 & 0 & 0 \\ C_{12} & C_{11} & C_{12} & 0 & 0 & 0 \\ C_{12} & C_{12} & C_{11} & 0 & 0 & 0 \\ 0 & 0 & 0 & C_{44} & 0 & 0 \\ 0 & 0 & 0 & 0 & C_{44} & 0 \\ 0 & 0 & 0 & 0 & 0 & C_{44} \end{vmatrix} \tag{5}$$

Note in equations 6, 7, 8 that the coefficients C_{11}, C_{12}, and C_{44} are expressed in terms of the elasticity modulus E and Poisson's ratio ν or Lame coefficients μ and λ.

$$C_{11} = \frac{E(1-\nu)}{(1+\nu)(1-2\nu)} = \lambda + 2\mu \tag{6}$$

$$C_{12} = \frac{E\nu}{(1+\nu)(1-2\nu)} = \lambda \tag{7}$$

$$C_{44} = \frac{E}{2(1+\nu)} = \mu = \frac{(C_{11} - C_{12})}{2} \tag{8}$$

Z axis is normal to the surface and parallel to cylindrical axis. The 3D model is meshed (Fig. 2(c)) into solid elements and solved using the finite element method (FEM) software COMSOL Multiphysics. The problem is solved using Eigen frequency and partial differential equation (PDE). The variation of wave vector in the first Brillouin Zone and the value of Eigen frequency for the first 20 harmonics are used to represent a dispersion band. For each natural frequency, the corresponding eigenvector can be calculated to show the spatial distribution and deformations of that mode, then the frequency dispersion curves as a function of the wave vectors k can be plotted in ΓX, XM and MΓ directions or MΓ, ΓX and XM directions.

3 Results and Discussion

In order to evaluate the effect of the pillars, we first calculate the band diagram of the model represented in Fig. 1(c) which corresponds to the specimen where the pillars of core and polymer do not emerge from a foundation of concrete ($h_1=h_2=h=t$). The reduced frequency dispersion curves $f.a$ (m/s) in terms of the reduced wave propagation factor k/a in half of the first Brillouin zone for this phase (material couple "steel-rubber") are shown in Fig. 3(a). Two very narrow band gaps appeared in relatively high frequencies. The relative widths of these band gaps are equal to 3.2% and 6.3%.

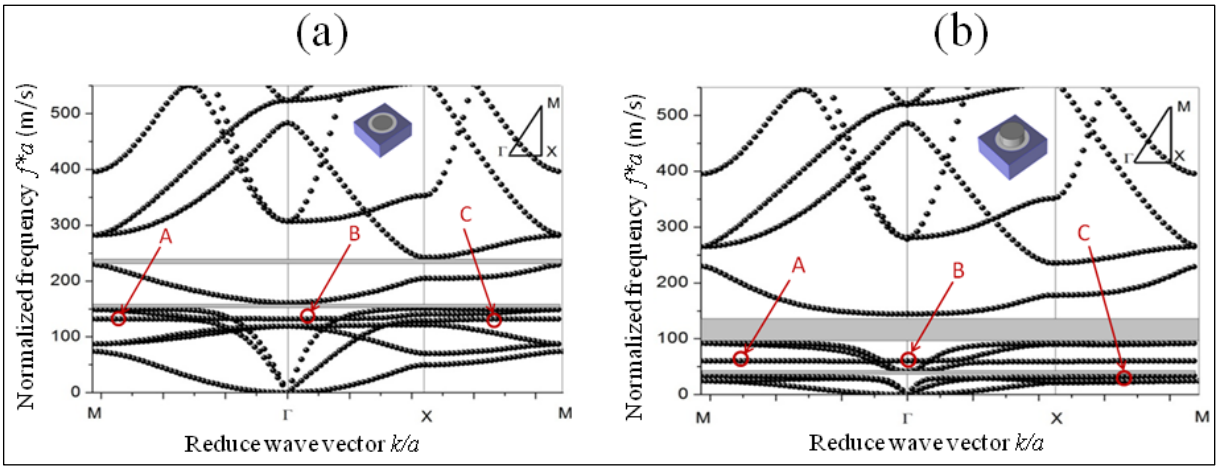

Fig. 3 – Frequency dispersion curves corresponding to "steel-rubber" material couple. (a) Pillars of steel and rubber not emerged from substrate of concrete ($r_1/a=0.45$; $r_2/a=0.35$; $h_1=h_2=t$); (Gaps between 155 - 160 m/s and 230 - 245 m/s). (b) Only pillar of steel emerged from substrate of concrete ($r_1/a=0.45$; $r_2/a=0.35$; $h_1=t$ and $h_2/a=0.5$); (Gaps between 35 - 40 m/s and 95 - 140 m/s)

In the second phase, the case where only pillars of core emerge from the substrate of concrete ($h_1=t$ *and* $h_2/a=0.5$) has been analysed. The results for the couple "steel-rubber" are illustrated in Fig. 3(b). A noticeable shift towards the low frequencies has been achieved together with an improvement in the relative widths of the band gap which have been widened to 13% and 38% for the first and the second band gap respectively. This is attributed to the resonance phenomenon that was highlighted by several researchers [21, 28, 35].

This resonance phenomenon can be illustrated on Fig. 4 where it can be seen that the three modes (A, B and C), localize energy in steel and polymer pillars.

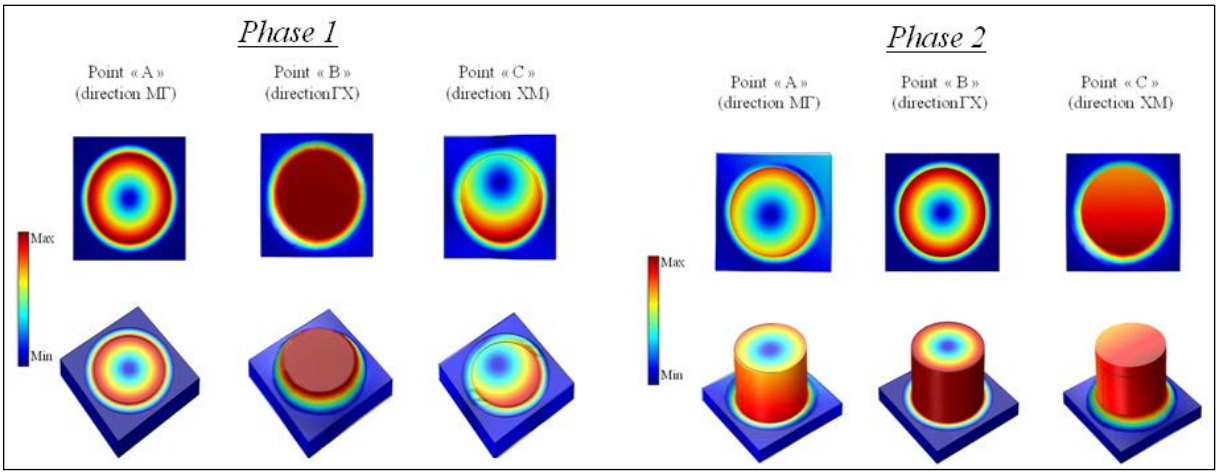

Fig. 4 – Locally resonance in cylinders steel for the first and second phases at A, B, C points.

In order to improve further these band gaps, a third phase has been carried out by increasing the dimension h_1. All pillars of metal core and polymer are emerged from the foundation of concrete. However, an optimization operation on the geometric

parameters of the model was made where all the relative geometric parameters of core and polymer cylinders (r_1/a, r_2/a, h_1/a and h_2/a) were varied (the dimension "a" is constant all time). It should be noted that this optimization operation is composed of four steps, in first time, r_1/a, r_2/a, h_1/a are kept unchanged and only h_2/a is varied. In second time, only h_1/a is varied and r_1/a, r_2/a, h_2/a are kept constant, etc.

Fig. 5 is an example of one step of frequency dispersion curve where r_1/a, r_2/a, h_1/a were kept constant and varied the relative dimension h_2/a. A medium gap appeared in the vicinity of 150 m/s. The radius and heights of metal and polymer were varied to achieve the best possible band gaps. For different pairs of materials, the relative dimensions r_1/a and r_2/a are respectively equal to 0.45 and 0.35; h_1/a and h_2/a have the same value as h/a and equal to 0.50.

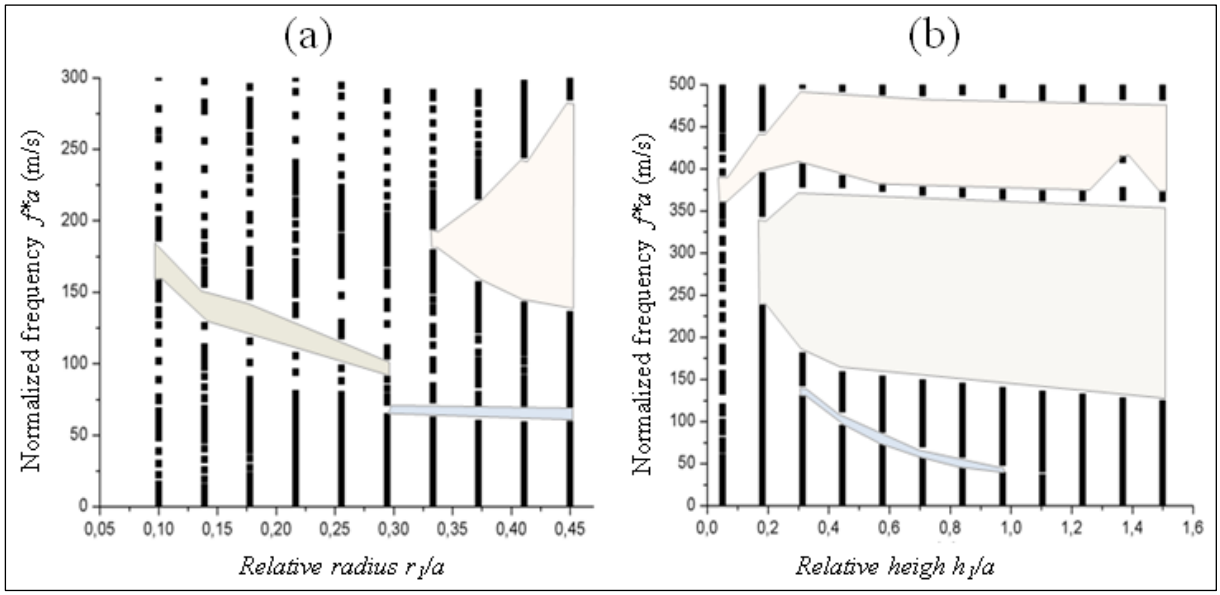

Fig. 5 – Frequency dispersion curves; materials used: concrete "steel-rubber". (a) all geometric parameters are constant; r_1/a is variable. (b) all geometric parameters are constant; h_1/a is variable.

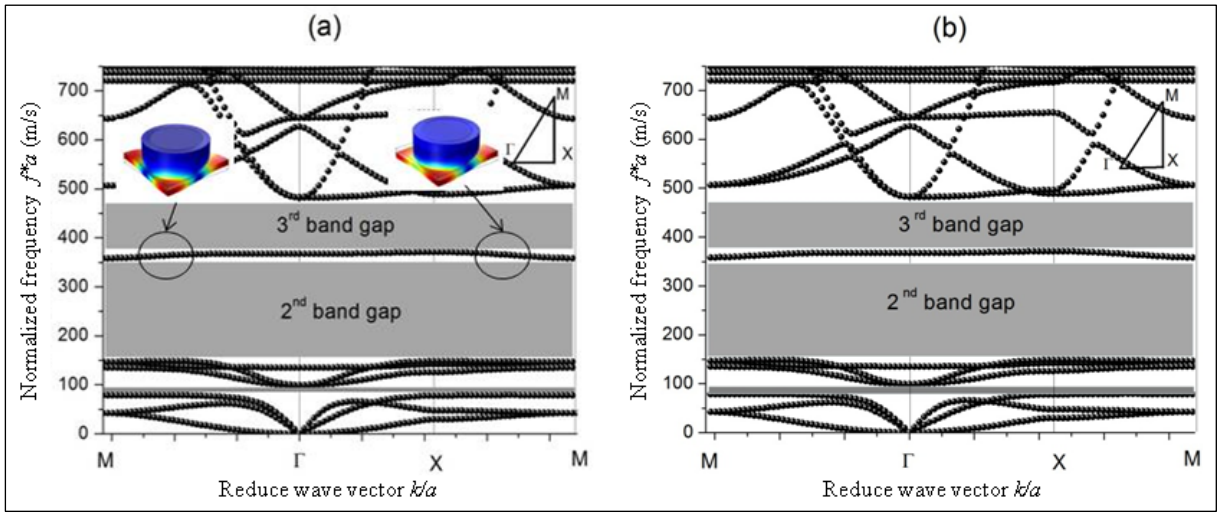

Fig. 6 – Frequency dispersion curves (r_1/a=0.45; r_2/a=0.35; h_1/a= h_2/a=0.5). (a) Materials used: concrete with "steel-pvc" (Gaps between 80 - 100 m/s, 150 - 350 m/s and 370 - 480m/s). (b) Materials used: concrete with "lead-pvc" (Gaps between 78 - 93 m/s, 150 - 350 m/s and 365 - 480m/s).

The band diagram for the two material couples "steel-PVC" and "lead-PVC" having three distinct band gaps are illustrated in Fig. 5. First, the emergence of metal core and polymer cylinders with the same height, led to a significant larger band gaps compared to the cases of Figs. 3(a) and 3(b) where both metal core and polymer doesn't emerge and only metal core emerge from substrate of concrete respectively. Secondly the effect of the difference of density of the metal core is not very significant (Figs. 5(a) and 5(b)), even though replacing steel by lead has slightly lowered the first band gap.

It can be also noticed in Fig. 5(a) that a relatively wide band gap ranges between 150 and 350 m/s while a third band is in the higher frequency range between 370 and 480 m/s; their relative widths are equal to 80% and 26%. A band gap at low frequency range appears between 80 and 100 m/s; its relative width is equal to 22.2%. The first band gap for the "lead-PVC" couple shown in Fig. 5(b) shifted towards a range between 78 and 93 m/s. This result is potentially attractive for civil engineering applications. Although the band gaps remain relatively high, the effect of contrast between materials can be used to adjust the band gaps.

In general, increasing the density of the metal core tends to lower the frequencies of the band gaps and creating high contrast between the densities of the metal core and the polymer increases the width of the band gaps. As can be seen in Fig. 5(b), the relative width of the band gaps increases by 5% for the third band, but it decreases by 25% for the first band when replacing the steel by lead. The second band gap is the same for both steel and lead.

The contrast of the density and stiffness between the materials used for the core and coating which is at the origin of the existence of these bands gap was underlined by many authors particularly Kushwaha et al. and Sigalas et al. [35, 36].

Taking advantage of this contrast effect an attempt is made to reach the seismic range of frequencies, by substituting the steel by lead and the PVC by rubber and then by silicone (Fig. 7).

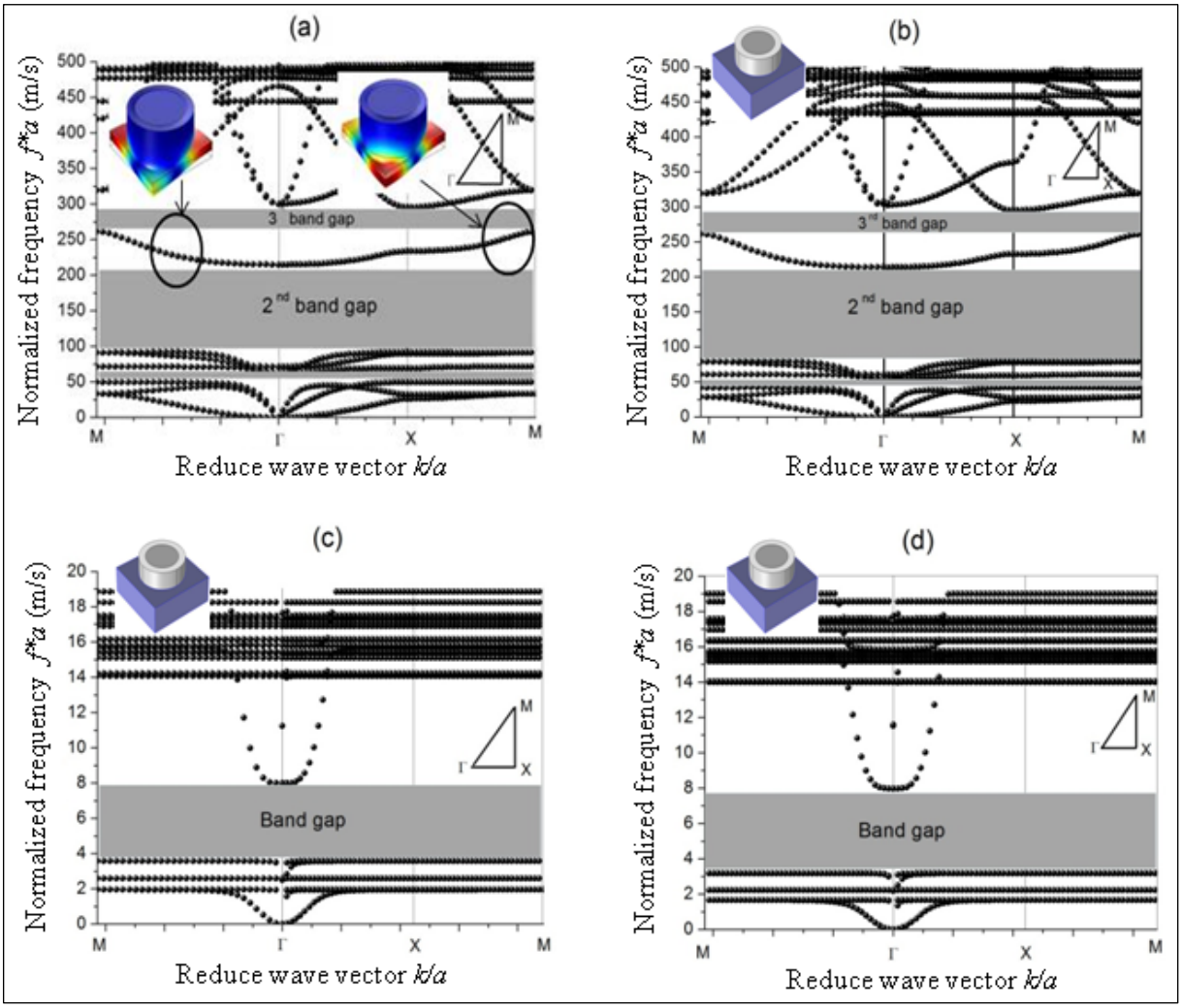

Fig. 7 – Effect of density contrast on the dispersion curves (r1/a=0.45; r2/a=0.35; h1/a=0.5; h2/a=0.5) and parasite modes vibrations. (a) Materials used concrete with "steel-rubber" (Gaps between 50 - 63 m/s, 93 - 215 m/s and 262 - 293 m/s).(b) Materials used concrete with "lead-rubber" (Gaps between 42 - 55 m/s, 82 - 212 m/s and 262 - 295 m/s). (c) Materials used concrete with "steel-silicone" (Gap between 3.6 - 8 m/s). (d) Materials used concrete with "lead-silicone" (Gap between 3.5 - 8 m/s)

When replacing the PVC by rubber (Fig. 7(a)), the centres of the first and third band gaps corresponding to the steel core shifted from 90 to 56.5 m/s and from 425 to 278.5 m/s respectively. Those of lead core translated from 85.5 to 48.5 m/s and from 422.5 to 328.5 m/s as shown in Fig. 7(b).

However, the use of silicone shows substantial drop of frequency band gaps because of its low elastic modulus. The influence of these parameters (density and elastic modulus) on the decrease of band gaps frequencies are also underlined by some authors especially Gaofeng et al. [34].

It should be noted that the band gaps corresponding to the steel as well as the lead core (Figs. 7(c) and 7(d)) become relatively similar even though that their characteristics in terms of elasticity and density are different; this can be attributed to the fact that the coating material (silicone) with very low elastic modulus turns out to be dominant at lower frequencies.

When the propagation of the elastic waves is constrained to the plane (XOY) perpendicular to the cylinders axes, then the elastic displacement vector $\vec{u}$ depends only on X and Y. On the basis of this hypothesis, the vibrations decoupled in modes of mixed polarization (or XY modes) and purely transverse modes (Z modes). The elastic displacement vector $\vec{u}$ for the XY modes is perpendicular to the cylinder axis $(\vec{u} \perp o\vec{z})$ while the Z modes ($\vec{u}$) are parallel to the cylinders.

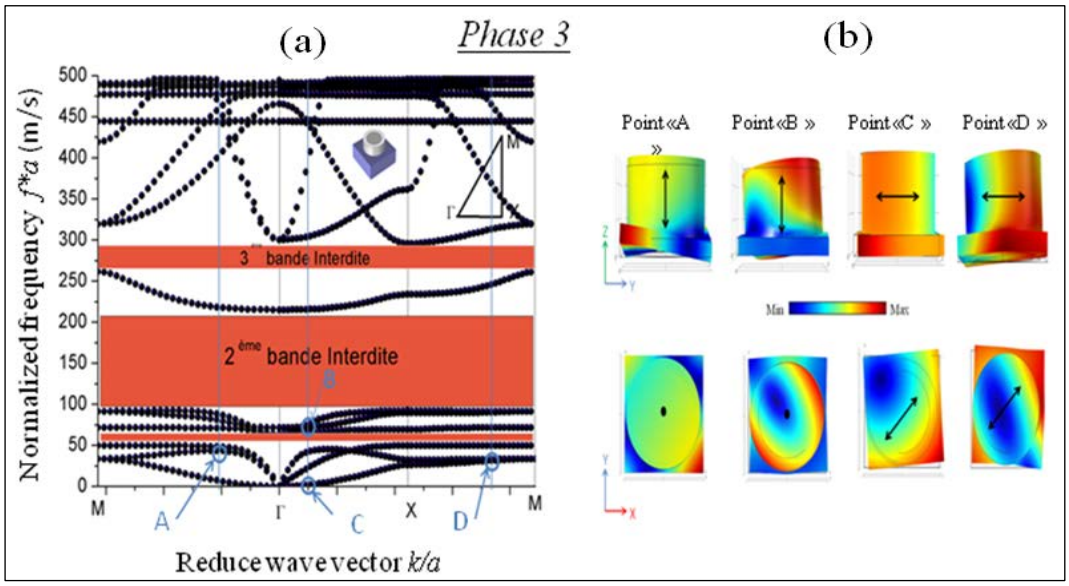

Fig. 8 – (a) Frequency dispersion curves (r_1/a=0.45; r_2/a=0.35; h_1/a= h_2/a=0.5). Materials used: concrete with "steel-rubber"; (b) Vibration modes of A, B, C, D points

we can clearly observe oscillations (points A and D) with displacements of the resonators parallel to the Z axis (Fig.8 (b), point A) or in the XY plane (Fig.8 (b), point D) accompanied by a bending of the concrete substrate (XY mode). On the other hand, for the points B and C, the oscillations cause displacements of the resonators parallel to the axis Z (Fig.8 (b), point B) or in the plane XY (Fig.8 (b), point C) accompanied by plane deformations of the substrate concrete (XY mode). Note that these deformations or displacements appear in the resonators but also extend for certain modes to the concrete substrate. It can be also noted a field of displacement outside the cylinders which shows a certain interaction between the substrate and the resonators; this demonstrates that this low frequency band gap can be dependent on the geometrical parameters of the substrate.

Fig. 9 summarizes the evolution of the first and third band gaps and their respective central frequencies with the material couples that have been used.

For bands with high frequencies (HBF) represented in Fig. 7(b), the decrease of the central frequencies is insignificant when increasing the density and elastic modulus of the metal. However, in the low frequencies (LBF) represented in Fig. 7(a), the central frequencies decrease significantly as the density and elasticity modulus of the metal increase. At very low frequencies, the two metals have practically the same behaviour when they are covered by silicone. Similarly, the quality factor shown in Fig. 8 presents the same trend.

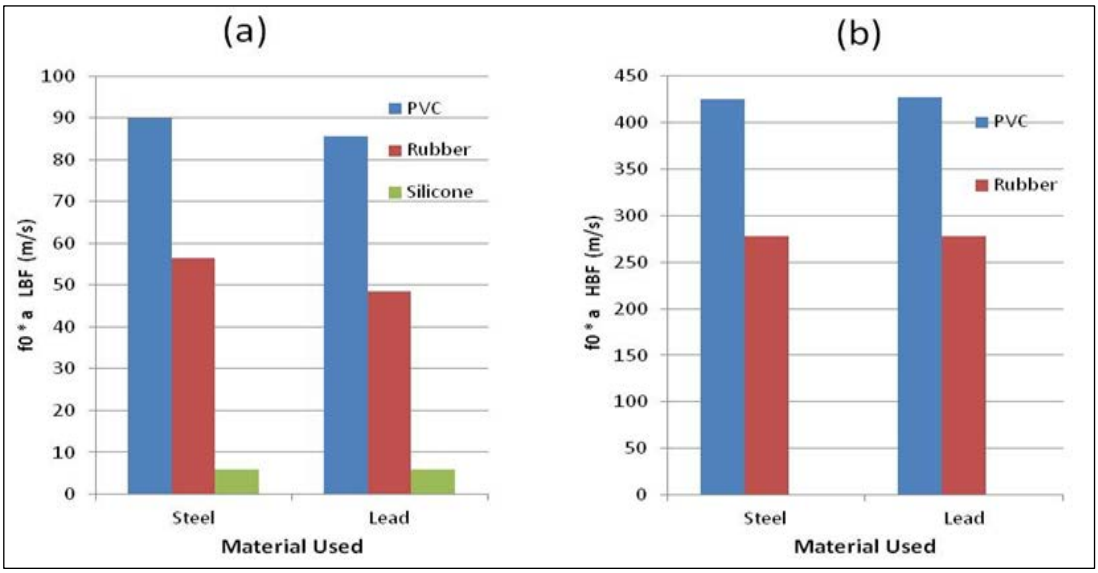

Fig. 9 – Central frequencies at low and high bands

Table 2 - Quality Factor $f_0/\Delta f$ (f_0 is the central frequency and Δf is the difference between the limits of the band gap).

	PVC		Rubber		Silicone	
	LBF	**HBF**	**LBF**	**HBF**	**LBF**	**HBF**
$f_0/\Delta f$ (Steel)	4.5	3.86	4.35	8.95	1.32	---
$f_0/\Delta f$ (Lead)	5.7	3.72	3.73	8.44	1.3	---

The Table 2 presents the values of the quality factor $f_0/\Delta f$ calculated for all pairs of materials that have been used. As shown in Fig. 8(a), the quality factor for (LBF) decreases when using sequentially PVC, rubber or silicone regardless of the metal used. In the contrary, the quality factor for (HBF) is better with the use of the rubber rather than PVC (Fig. 8(b)).

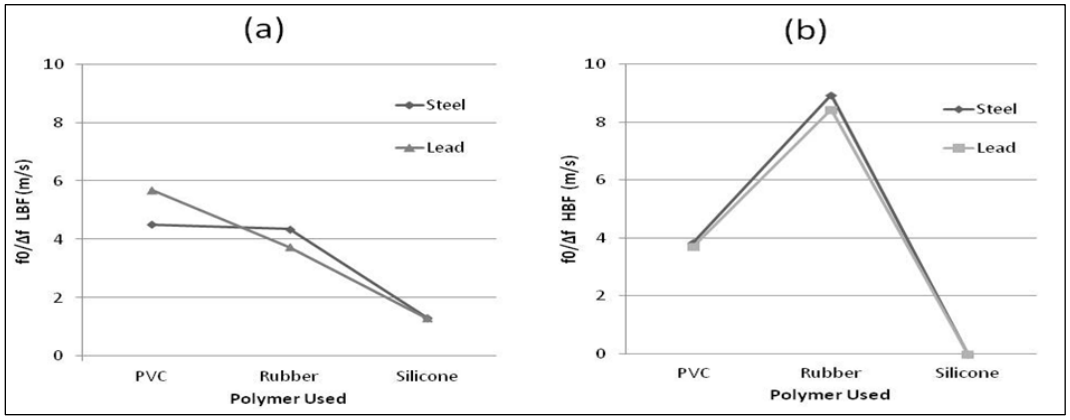

Fig. 10 – Quality Factors of Central frequencies at low (LBF) and high (HBF) bands.

It should be noted that in Figs. 5 and 6, the 2nd and 3rd band gaps are separated by frequency borders that lay around 350 and 230 m/s for PVC and rubber respectively.

When considering the polarization of the upper bound frequency of the band gap for different pairs of materials, particularly the couples "steel-PVC" or "steel-rubber", it has been found that the vibration energy corresponding to these modes is concentrated at the corners of the concrete foundation as illustrated by circles in Figs. 6(a) and 8(a). These deformations correspond to *k* equal to 2.54 and 1.51 for Fig. 6(a) and 2.05 and 3 for Fig. 8(a). These modes have a high amplitudes at the corners of the unit where two opposite corners vibrate in phase and the two others vibrate out of phase [32].

To prevent these vibration modes, a new unit cell has been created by making notches at corners of the concrete foundation as shown in Fig. 2(d).

However, it is useful to specify that these modes of vibration are not necessarily dangerous for the structure; but the fact that they are concentrated at the corners of the cell unit, it suggests to explore the effect of notching the ends.

As reported in recent study [32] that making notches at corners of the concrete substrate (phase 4) shifted the band gaps towards lower frequencies for most couples of materials.

The frequency dispersion curves of the notched model (phase 4) in comparison with model before notching (phase 3) are plotted in Fig. 11. Two different effects can be noticed. For the "steel-pvc" couple, the width of the band gaps have been reduced and shifted towards lower frequencies (Figs. 11(a) and 11(b)). However, the third band gap of the "steel-rubber" couple gained about 30% in width and shifted towards lower frequencies (Figs. 11(c) and 11(d)). The first and the second band gap particularly for the couple "steel-rubber" did not change.

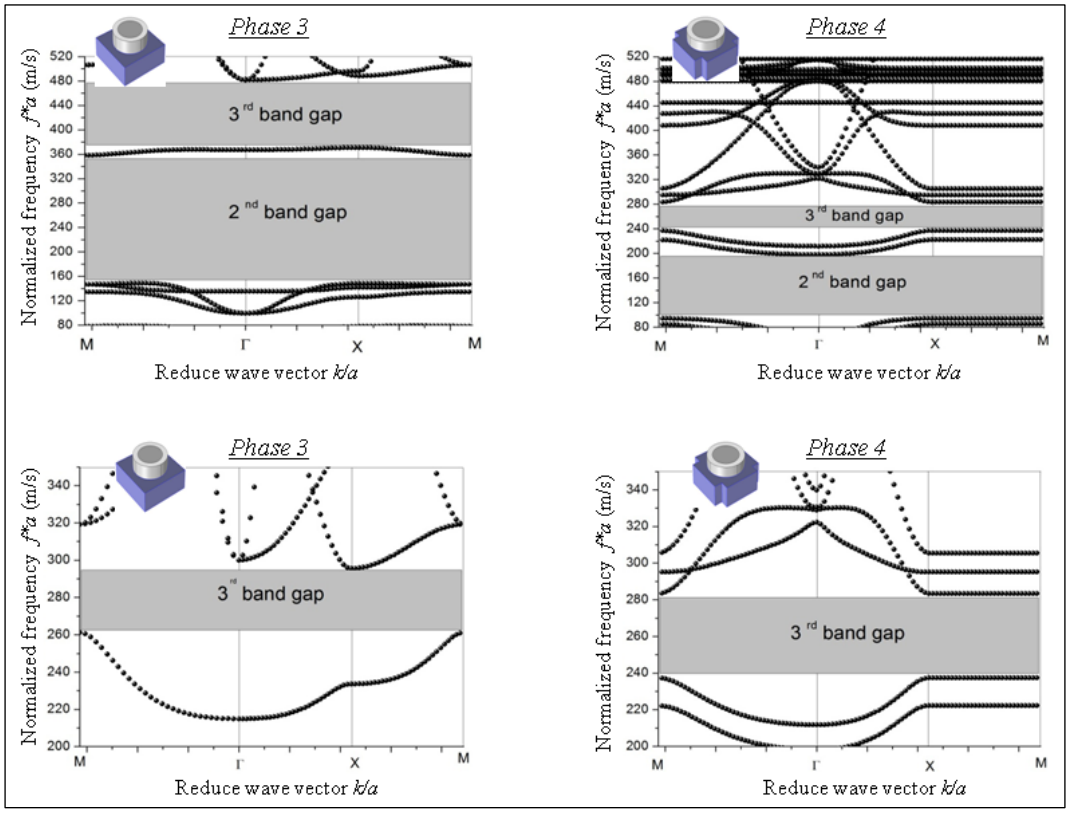

Fig. 11– Frequency dispersion curves of the notched models. (a) "steel-pvc" couple (phase 3), (b) "steel-pvc" couple (phase 4). (c) "steel-rubber" couple (phase 3), (d) "steel-rubber" (phase 4)

Considering the above results, in terms of width of band gaps and the corresponding central frequencies, if a dimension "*a*" of the concrete foundation equal to 1 meter, so it's would generate band gaps between 3.5 and 100 Hz for different material couples. These frequencies ranges can be potentially suitable for some practical solutions to isolate the propagation of seismic vibrations or vibrations from industrial equipments.

Moreover, it is important to note that the dispersion curves have, in the ΓX direction of the Brillouin zone, three low frequency branches characteristic of Lamb modes for a homogeneous plate.

We clearly distinguish the modes A_0, S_H and S_0, antisymmetrical, transverse horizontal and symmetrical respectively, characterized by the branches 1, 2 and 3.

This is to confirm that the appearance of a phononic band gap is the direct consequence of coupling in the band structure between Lamb modes and localized modes.

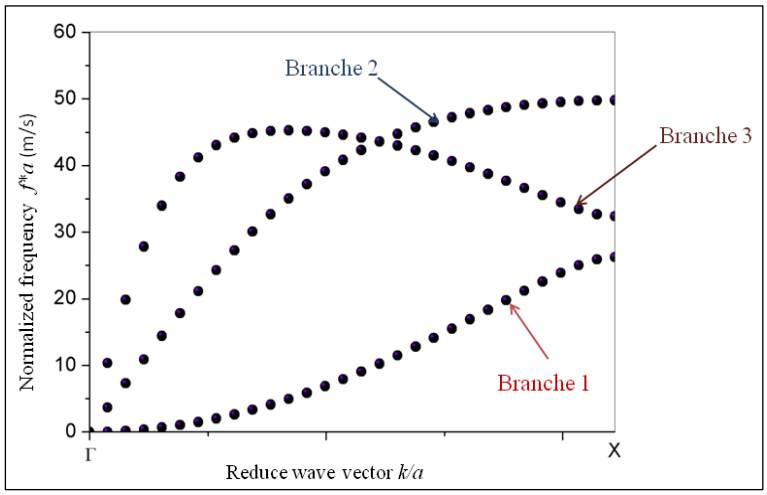

Fig. 12– Lamb's modes in a first direction of Brillouin's irreducible zone

To investigate the effect of the thickness ratio *t/a*, four values equal to 0.10, 0.30, 0.50 and 0.90 are considered. For all these values, the emergence of the cylinders is maintained constant. The Figure 13 illustrates the evolution of the structure of the dispersion curves of the eigen frequencies as a function of the relative thickness of the concrete substrate.

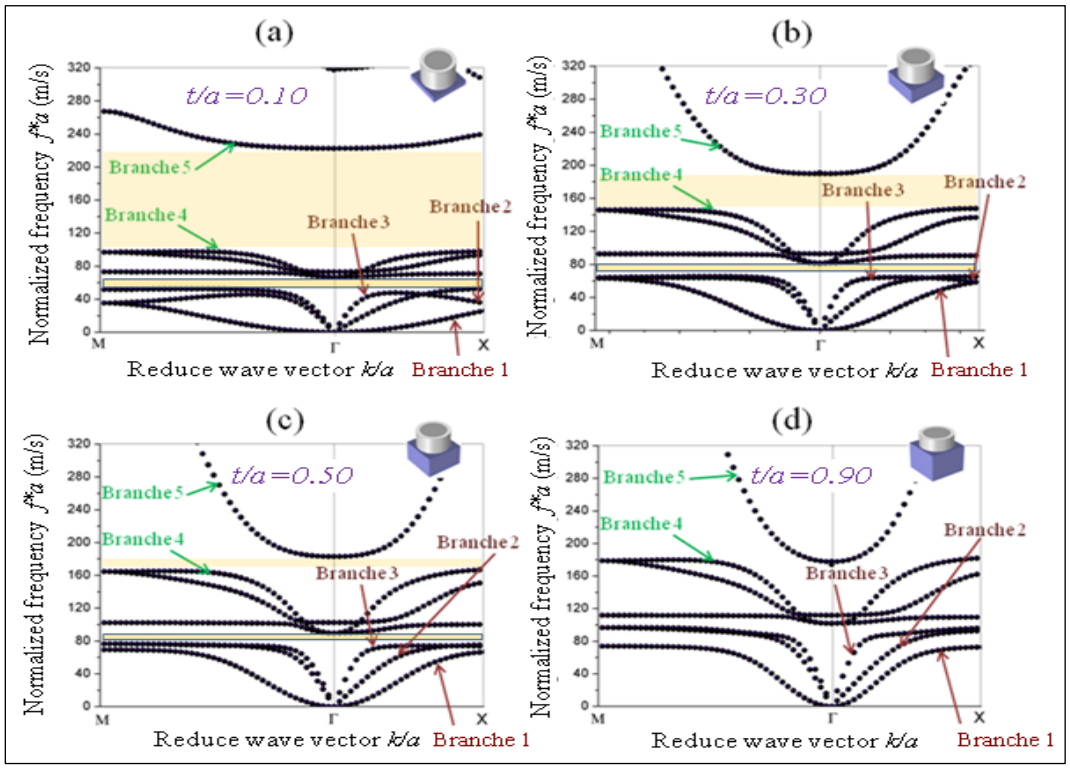

Fig. 13– Frequency dispersion curves (r_1/a=0.45; r_2/a=0.35; h_1/a= h_2/a=0.5) when relative thickness of concrete substrate t/a is variable and equal to 0.10, 0.30, 0.50 and 0.90; Materials used: concrete with "steel-rubber"

Fig. 13 shows the existence of Lamb modes through branches 1, 2 and 3, even when the relative thickness of the concrete substrate becomes important and approaches the unity. It can be also seen on this figure that the lowest dispersion curves and the first band gap are moving towards the higher frequencies as the thickness of the substrate increases. Similarly, the branches 1, 2 and 3 corresponding to the Lamb modes evolve rather slowly upwards (branch 3 more quickly than the other two). This slow evolution contributes to the preservation of the first band gap; even if the width of the latter becomes smaller and smaller while shifting towards the high frequencies. On the other hand, when one looks closely at the evolution of the branch 5, it could be noticed clearly also that the bending of the latter is more important for large values of the relative

thickness. This bending causes the two branches 4 and 5 to get closer together, while narrowing the width of the second gap band, until it disappears completely when the relative thickness reaches the value 0.9. This result has been pointed out by some researchers [32, 38] who consider that, as a general rule, the increase in the relative thickness of the substrate leads to a reduction in the cut off frequencies of the higher order modes of the substrate, thus causing the closure band gaps of low frequencies.

However, when the relative thickness of the concrete substrate is varied, the height of the emergent portion of the cylinders inevitably changes, which may be similar to a simultaneous variation in the thickness of the concrete substrate and the height of the resonators. Therefore, this time we will fix the relative thickness of the concrete substrate at 0.10 and we will take the relative height of the steel and rubber rolls equal to 0.25, 0.35, 0.50 and 0.75. Figure 14 shows the frequency dispersion curves as a function of the wave vector in the ΓX direction.

It can be noted on this figure that the existence, the position and the width of the first band gap (band in yellow color) show an obvious dependence of the height of the resonators. The increase of the latter causes a shift of the band gap towards the low frequencies and expand it. The improvement of the band gap is such that the relative widths increase gradually from 2%, 10%, 23% to 33%, when the relative heights are equal to 0.25, 0.35, 0.50 and 0.75 respectively.

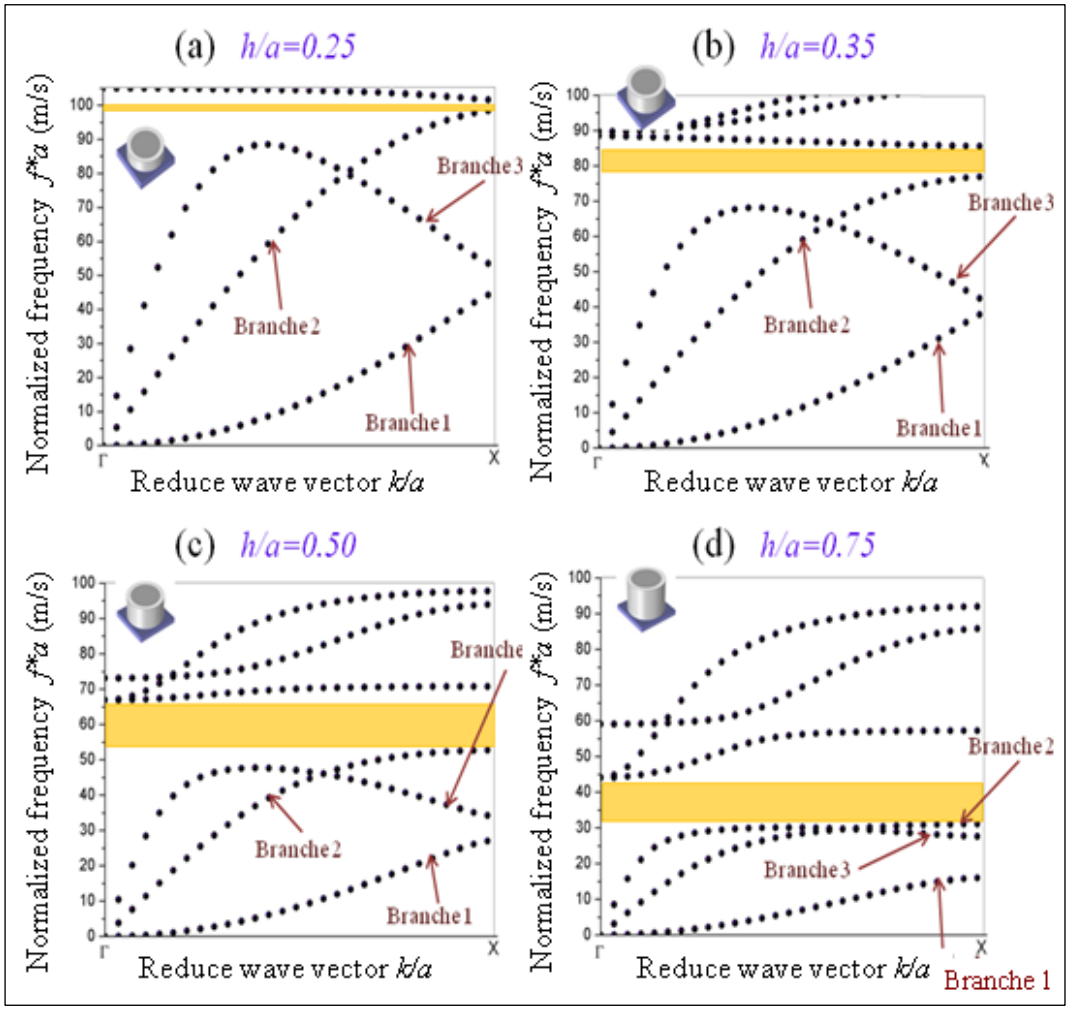

Fig. 14– Frequency dispersion curves (r_1/a=0.45; r_2/a=0.35; t/a=0.10) when relative height h/a of resonators is variable and equal to 0.25, 0.35, 0.50 and 0.75; Materials used: concrete with "steel-rubber"

Figures (14 (a) to 14 (d)) show that the lower bound of this band gap is limited by the branch 2 which represents the horizontal shear mode (S_H) of Lamb. Indeed, the increase of the relative height *h/a* is at the origin of the increasingly important bending of the branch 2, which is in fact responsible for the opening of the band gap and its sliding towards the low frequencies. Therefore, in the light of these results and in view of the distribution of the displacement fields between the

resonators and the concrete substrate, it can be deduced that the existence of the low frequency band gaps is not related exclusively to the resonance phenomenon, but also to the movement and bending of the characteristic branches of the Lamb modes of a homogeneous plate. This conclusion has also been advanced by several authors [19,39]. It can be deduced from the figures 13 and 14 that the two geometrical parameters *t* and *h* are antagonistic, so that a good choice of the pair of values (*t*, *h*) must be made in order to have an acceptable band gap width.

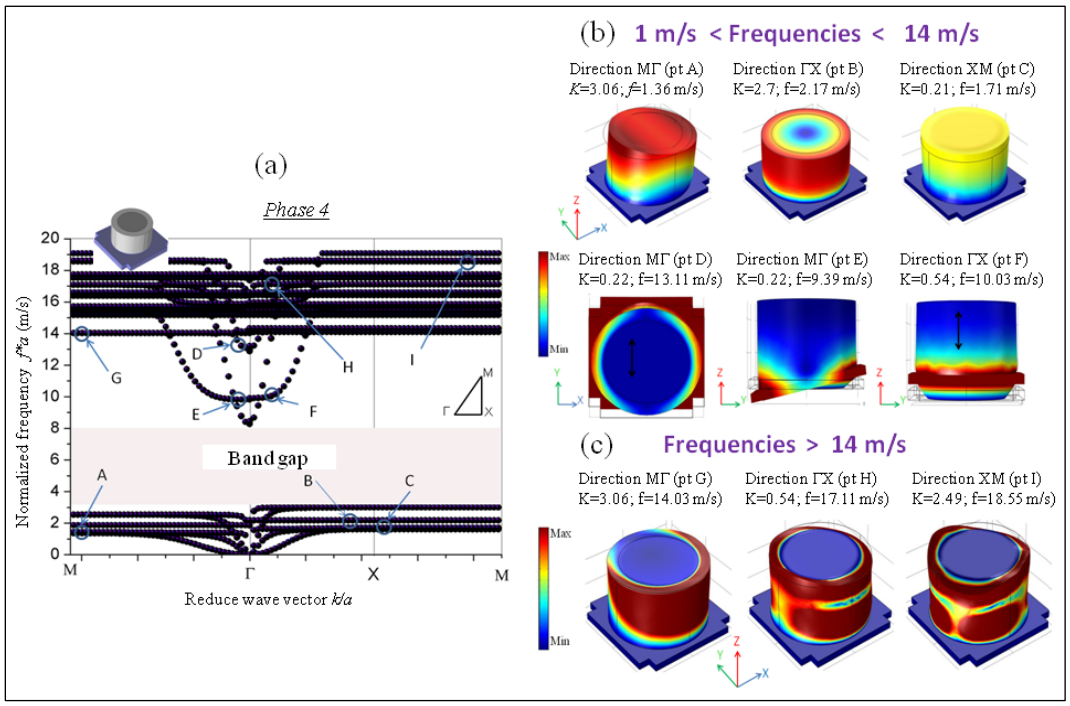

Fig. 15– (a) Frequency dispersion curves (phase 4); Materials used: concrete with "steel-silicone"; (b)Vibration modes at A, B, C, D, E, F points (1<f*a<4m/s); (c) Vibration modes at G, H, I points (f*a > 14m/s)

After making notches at the corners of the concrete substrate [32], for the couple of materials "steel--silicone", the frequencies dispersion curves is presented in Fig. 15(a). By analyzing the different branches of this figure corresponding to the low frequencies (frequencies lower than 4 m/s), we note that the vibrations are localized at the cylinders which corresponds to local resonance modes (points A, B and C) as shown in Figure 15(b). The branches relating to the frequencies between 4 and 14 m/s correspond to vibration modes concentrated in the concrete substrate (Fig. 15(b), points D, E and F); these modes are modes of translation parallel to Y and Z (points D and F) or flexion (point E). In fact, this Lamb's mode A_0 (antisymmetric or "Flexural"), has a strong out of plane component, but also a small in the plane component; it can therefore strongly couple with localized modes in plane or with transverse localized modes. Also, it is noted that frequencies greater than 14 m/s generate concentrated vibration modes in the polymer layer only as illustrated in Figure 15(c).

It is recalled in this model that the relative radius of the steel core and the polymer (silicone) are r_2/a = 0.35 and r_1/a = 0.45 respectively which gives us a silicone thickness of 0.10 m. If we reduce the thickness of the silicone layer to 5 cm, we obtain frequencies of dispersion curve represented in Fig. 16(b) in comparison with that obtained before notching (Fig. 16(a)).

A very interesting result obtained by the decrease of thickness of the silicone from 10 to 5 cm, is illustrated in Figure 16 which shows two band gaps between 3.8 and 8 m/s for the initial model before notching (phase 3) and 11 m/s for the model after notching (phase 4). The width of the band gap passes from 4.2 to 7 m/s; a gain in width is evaluated about 67%.

Further reduction of the thickness of the silicone layer to 2.5 cm led to frequency dispersion curves characterized by a shift of the frequency branches above 8 m/s towards the high frequencies as shown on Fig. 17. Nevertheless an important gain in the width of a band gap between 5.5 and 14 m/s is obtained at a relatively higher frequency center which rises from 5.9 to 9.75 m/s; a gain in width is evaluated about 100%.

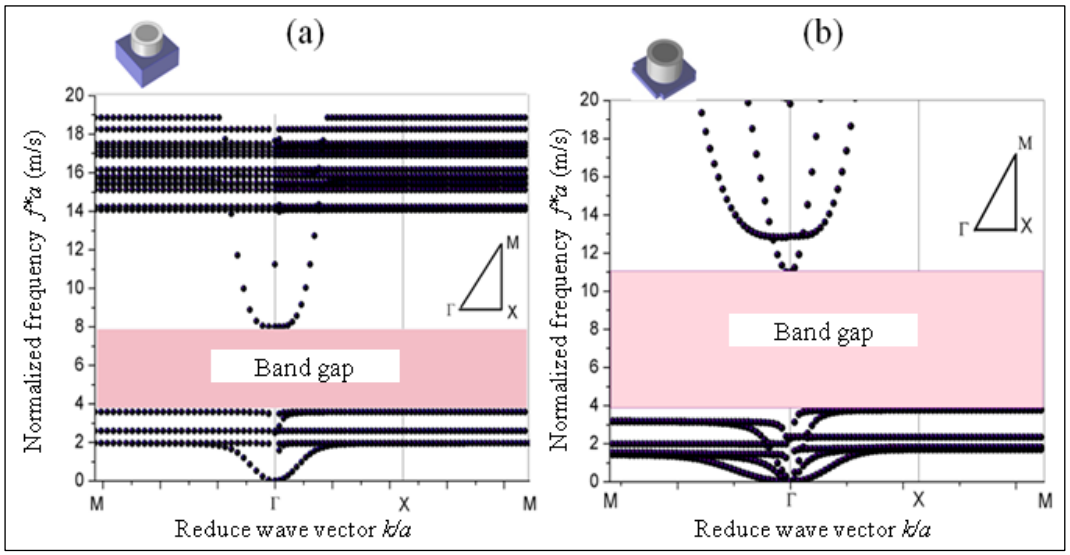

Fig. 16– Frequency dispersion curves Materials used: concrete with "steel-rubber" (a) Basic model (phase 3, $r_1/a=0.45$; $r_2/a=0.35$; $h_1=h_2=0.50$); (b) Basic model after notching (phase 4, $r_1/a=0.45$; $r_2/a=0.40$; $h_1=h_2=0.50$);

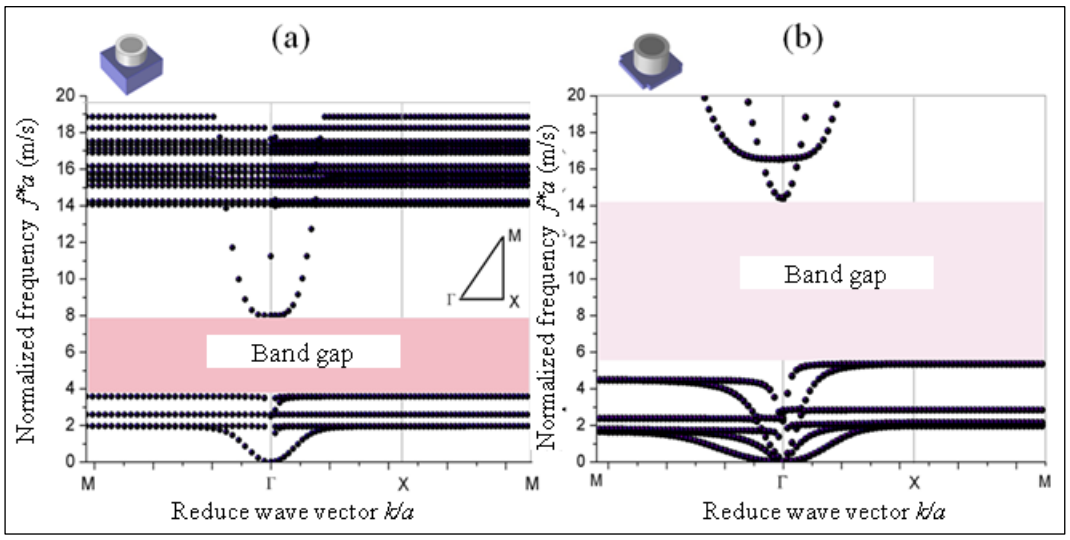

Fig. 17– Frequency dispersion curves Materials used: concrete with "steel-rubber" (a) Basic model (phase 3, $r_1/a=0.45$; $r_2/a=0.35$; $h_1=h_2=0.50$); (b) Basic model after notching (phase 4, $r_1/a=0.45$; $r_2/a=0.425$; $h_1=h_2=0.50$)

4 Conclusion

The concept of periodic networks did gain a strong foothold in many fields of practical applications in engineering. Because of the very low frequency range of seismic vibration, the use of this technique to mitigate the effect of earthquake vibrations is still a challenging task. In this context, a feasibility study is undertaken to investigate the efficiency in creating band gaps at low frequencies using common construction materials. Concrete blocks inlaid with steel or lead pillars coated in PVC, rubber or silicone in different configurations has been used as an isolation system. Band gaps at medium and low frequencies have been achieved for some combination of materials. The difference of density and elasticity of metal core is not very significant when we replace steel by lead. Some of these band gaps have been widened (for rubber) and translated towards low frequencies (for pvc and rubber) by notching the corners of the basic models with these polymers coating. In the ΓX direction, all the dispersion curves show three characteristic branches of the Lamb modes even when the relative thickness of the concrete substrate becomes large and approaches the unity. The analysis of the frequency dispersion curves as a function of the thickness of the concrete and the height of the metal and polymer cylinders, has shown that the existence of band gaps at low frequencies and their opening, are generated by the displacement and curvature of the branches representing

the Lamb modes, particularly the branches 2 and 3 corresponding to the horizontal shear mode (S_H) and the symmetrical mode (S_0). It can be also deduced that the two geometrical parameters *t* and *h* are antagonistic, so that a good choice of the pair of values (*t, h*) must be made in order to have an acceptable band gap width. The frequency range and the width of the obtained band gaps can be suitable for mitigating seismic and industrial induced vibrations in civil engineering structures.

REFERENCES

[1]- F. Casciati, L. Faravelli, K. Hamdaoui, Performance of a base isolator with shape memory alloy bars. Earthq. Eng. Eng. Vib. 6(4) (2007) 401-408. doi:10.1007/s11803-007-0787-2

[2]- J.G. Kang, B. S. Kang, Dynamic analysis of fiber-reinforced elastomeric isolation structures. J. Mech. Sci. Technol. 23(4) (2009) 1132–1141. doi:10.1007/s12206-008-1214-y

[3]- A. Jalali, D. Cardone, P. Narjabadifam, Smart restorable sliding base isolation system. Bull. Earthquake Eng. 9(2) (2011) 657–673. doi:10.1007/s10518-010-9213-7

[4]- O.E. Ozbulut, S. Hurlebaus, Fuzzy control of piezoelectric friction dampers for seismic protection of smart base isolated buildings. Bull. Earthquake Eng. 8(6) (2010)1435–1455. doi:10.1007/s10518-010-9187-5

[5]- X. Li, S. Xue, Y. Cai, Three-dimensional seismic isolation bearing and its application in long span hangars. Earthq. Eng. Eng. Vib. 12(1) (2013) 55-65. doi:10.1007/s11803-013-0151-7

[6]- A. Bakhshi, M.H. Jafari, V.V. Tabrizi, Study on dynamic and mechanical characteristics of carbon fiber- and polyamide fiber-reinforced seismic isolators. Mater. Struct. 47(3) (2014) 447–457. doi:10.1617/s11527-013-0071-z

[7]- P.M. Calvi, D.M. Ruggiero, Numerical modelling of variable friction sliding base isolators. Bull. Earthquake Eng. 14(2) (2016) 549–568. doi:org/10.1007/s10518-015-9834-y

[8]- J.W. Hu, Seismic analysis and parametric study of SDOF lead-rubber bearing (LRB) isolation systems with recentering shape memory alloy (SMA) bending bars. J. Mech. Sci. Technol. 30(7) (2016) 2987-2999. doi:10.1007/s12206-016-0608-5

[9]- G.P. Lignola, L. Di Sarno, M. Di Ludovico, A. Prota, The protection of artistic assets through the base isolation of historical buildings: a novel uplifting technology. Mater. Struct. 49(10) (2016) 4247–4263. doi:10.1617/s11527-015-0785-1

[10]- Q. Li, Y. Zhu, D. Xu, J. Hu, W. Min, L. Pang, A negative stiffness vibration isolator using magnetic spring combined with rubber membrane, J. Mech. Sci. Technol. 27 (3) (2013) 813-824. doi:10.1007/s12206-013-0128-5

[11]- Y. Lai, Z.Q. Zhang, Large band gaps in elastic phononic crystals with air inclusions. Appl. Phys. Lett. 83(19) (2003) 3900. doi:10.1063/1.1625998

[12]- J. Gao, X.Y. Zou, J.C. Cheng, B. Li, Band gaps of lower-order Lamb wave in thin plate with one-dimensional phononic crystal layer: Effect of substrate. Appl. Phys. Lett. 92 (2) (2008) 023510. doi:10.1063/1.2834700

[13]- W. Xiao, G.W. Zeng, Y.S. Cheng, Flexural vibration band gaps in a thin Plate containing a periodic array of hemmed discs. Applied Acoustics. 69(3) (2008) 255–261. doi:10.1016/j.apacoust.2006.09.003

[14]- Y. Pennec, B.D. Rouhani, H. Larabi, A. Akjouj, J.N. Gillet, J.O. Vasseur, G. Thabet, Phonon transport and wave guiding in a phononic crystal made up of cylindrical dots on a thin homogeneous plate. Physical Review B. 80 (2009) 144302. doi:10.1103/PhysRevB.80.144302

[15]- Y. M. Soliman, M.F. Su, Z.C. Leseman, C.M. Reinke, I. El-Kady, R.H. Olsson, Phononic crystals operating in the gigahertz range with extremely wide band gaps. Appl. Phys. Lett. 97, (2010), 193502. doi:10.1063/1.3504701

[16]- H.J. Xiang, Z.F. Shi, S.J. Wang, Y.L. Mo, Vibration Attenuation and Frequency Band Gaps in Layered Periodic Foundation: Theory and Experiment. In: Proceedings of the 15th World Conference on Earthquake Engineering 2012 (15WCEE), Lisbon, (2012) , pp. 3831-3839.

[17]- H. Lv, X. Tian, M.Y. Wang, D. Li, Vibration energy harvesting using a phononic crystal with point defect states, Appl Phys. Lett. 102 (2013) 034103. doi:10.1063/1.4788810

[18]- F.L. Hsiao, A. Khelif, H. Moubchir, A. Choujaa, C.C. Chen, L. Laude, Complete band gaps and deaf bands of triangular and honeycomb water-steel phononic crystals. Appl. Phys. Lett. 101 (2007) 044903. doi:10.1063/1.2472650

[19]- Y. Pennec, J.O. Vasseur, B. Djafari-Rouhani, L. Dobrzyński, P.A. Deymierb, Two-dimensional phononic crystals: Examples and applications. Surface Science Reports. 65(8) (2010) 229–291. doi:10.1016/j.surfrep.2010.08.002

[20]- S. Mohammadi, A.A. Eftekhar, A. Khelif, W.D. Hunt, A. Adibi, Evidence of large high frequency complete

phononic band gaps in silicon phononic crystal plates. Appl. Phys. Lett. 92(22) (2008) 221905. doi:10.1063/1.2939097

[21]- A. Khelif, Y. Achaoui, S. Benchabane, V. Laude, B. Aoubiza, Locally resonant surface acoustic wave band gaps in a two-dimensional phononic crystal of pillars on a surface. Physical Review B. 81 (2010) 214303. doi:10.1103/PhysRevB.81.214303

[22]- H. Khales, A. Hassein-Bey, A. Khelif, Evidence of Ultrasonic Band Gap in Aluminum Phononic Crystal Beam. J. Vib. Acoust. 135(4) (2013) 041007. doi:10.1115/1.4023827

[23]- Y. Yan, A. Laskar, Z. Cheng, F. Menq, Y. Tang, Y.L. Mo, Z. Shi, Seismic isolation of two dimensional periodic foundations. Journal of Applied Physics. 116(4) (2014) 044908. doi:10.1063/1.4891837

[24]- Z.B. Cheng, Z.F. Shi, H.J. Xiang, Vibration Attenuation by Periodic Foundations. In: Proceedings of the 15th World Conference on Earthquake Engineering 2012 (15WCEE), Lisbon, 2012, pp. 23626-23635.

[25]- J.C. Hsu, Local resonances-induced low-frequency band gaps in two-dimensional phononic crystals labs with periodic stepped resonators. Phys. D: Appl. Phys. Lett. 44 (2011) 055401 . doi:10.1088/0022-3727/44/5/055401

[26]- A. Khelif, S. Mohammadi, A.A. Eftekhar, A. Adibi, B. Aoubiza, Acoustic confinement and wave guiding with a line-defect structure in phononic crystal Slabs. Appl. Phys. Lett. 108(8) (2010) 084515. doi:10.1063/1.3500226

[27]- M. Oudich, M.B. Assouar, Z. Hou, Propagation of acoustic waves and wave guiding in a two dimensional locally resonant phononic crystal plate, Appl. Phys. Lett. 97(19) (2010) 193503. doi:10.1063/1.3513218

[28]- Y. Achaoui, A. Khelif, S. Benchabane, L. Robert, V. Laude, Experimental observation of locally-resonant and Bragg band gaps for surface guided waves in a phononic crystal of pillars. Phys. Rev. B. 83(10) (2011) 104201. doi:10.1103/PhysRevB.83.104201

[29]- M. B. Assouar, M. Oudich, Enlargement of a locally resonant sonic band gap by using double-sides stubbed phononic plates. Appl. Phys. Lett. 100(12) (2012) 123506. doi:10.1063/1.3696050

[30]- J. Jiahong Ma, Z. Hou, B.M. Assouar, Opening a large full phononic band gap in thin elastic plate with resonant units. J. Appl. Phys. 115(9) (2014) 093508. doi:10.1063/1.4867617

[31]- P.R. Wagner, V.K. Dertimanis, E.N. Chatzi, I.A. Antoniadis, Design of Metamaterials for Seismic Isolation. In: Proceedings of the 34th IMAC, A Conference and Exposition on Structural Dynamics 2016. Dynamics of Civil Structures, 2016, pp. 275–287. doi:10.1007/978-3-319-29751-4

[32]- A. Amrane, N. Bourahla, A. Hassein bey, A. Khelif, Protection of structures subject to seismic and mechanical vibrations using periodical networks. Mod. Ar. Rev. Fund. Appl. Phys. 2(1) (2017) 29-32.

[33]- A. Khelif, B. Aoubiza, S. Mohammadi, A. Adibi, V. Laude, Complete band gaps in two-dimensional phononic crystal slabs. Phys. Rev. E. 74(4) (2006) 046610. doi:10.1103/PhysRevE.74.046610

[34]- J. Gaofeng, S. Zhifei, A new seismic isolation system and its feasibility study. Earthq. Engin. Engin. Vib. 9 (1) (2010) 75-82. doi:10.1007/s11803-010-8159-8

[35]- Y. Pennec, B.D. Rouhani, H. Larabi, J.O. Vasseur, A.C. Hladky-Hennion, Low-frequency gaps in a phononic crystal constituted of cylindrical dots deposited on a thin homogeneous plate. Phys. Rev. B. 78(10) (2008) 104105. doi:10.1103/PhysRevB.78.104105

[36]- M.S. Kushwaha, P. Halevi, G. Martinez, L. Dobrzynski, B.D. Rouhani, Theory of acoustic band structure of periodic elastic composites. Phys. Rev. B. 49(4) (1994) 2313. doi: 10.1103/PhysRevB.49.2313

[37]- M. Sigalas, M.S. Kushwaha, E.N. Economou, M Kafesaki, I.E. Psarobas, W. Steurer, Classical vibrational modes in phononic lattices: theory and experiment. Crystalline Materials. 220(9-10) (2005) 765–809. doi:10.1524/zkri.2005.220.9-10.765

[38]- B. Djafari-Rouhani, Y. Pennec, H. Larabi, J. Vasseur, A.C. Hladky, Band gaps in a phononic crystal constituted by cylindrical dots on a homogeneous plate. J. Acoustical Soc. Am. 123(5) (2008) 3041. doi:10.1121/1.2932724

[39]- M. Oudich, Y. Li, B.M. Assouar, Z. Hou, A sonic band gap based on the locally resonant phononic plates with stubs. New J. of Phys. 12(2010) 083049. doi:10.1088/1367-2630/12/8/083049